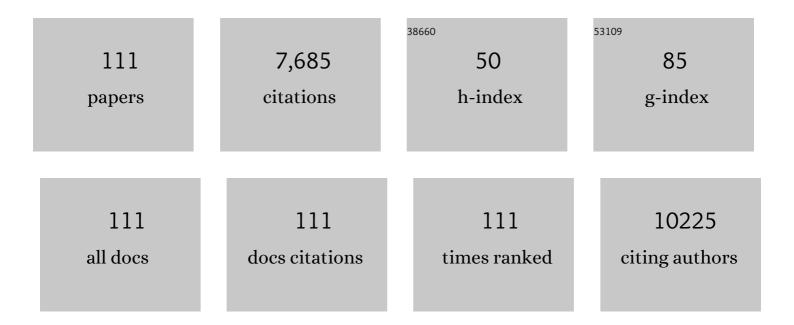
Daqiang Gao

List of Publications by Year in descending order

Source: https://exaly.com/author-pdf/6322342/publications.pdf Version: 2024-02-01



#	Article	IF	CITATIONS
1	Atomic-level coupled spinel@perovskite dual-phase oxides toward enhanced performance in Zn–air batteries. Journal of Materials Chemistry A, 2022, 10, 1506-1513.	5.2	28
2	Significant Change of Metal Cations in Geometric Sites by Magneticâ€Field Annealing FeCo ₂ O ₄ for Enhanced Oxygen Catalytic Activity. Small, 2022, 18, e2104248.	5.2	21
3	High efficiency electrocatalyst of LaNiO3@LaCoO3 nanoparticles on oxygen-evolution reaction. FlatChem, 2022, , 100371.	2.8	0
4	Fluorination activates the basal plane HER activity of ReS ₂ : a combined experimental and theoretical study. Journal of Materials Chemistry A, 2021, 9, 14451-14458.	5.2	21
5	Optimized Conductivity and Spin States in N-Doped LaCoO ₃ for Oxygen Electrocatalysis. ACS Applied Materials & Interfaces, 2021, 13, 2447-2454.	4.0	34
6	S-doped CoMn2O4 with more high valence metallic cations and oxygen defects for zinc-air batteries. Journal of Power Sources, 2021, 491, 229584.	4.0	40
7	Fe13+-ion irradiated WS2 with multi-vacancies and Fe dopants for hydrogen evolution reaction. FlatChem, 2021, 27, 100247.	2.8	3
8	Cr cation-anchored carbon nanosheets: synthesis, paramagnetism and ferromagnetism. Nanotechnology, 2021, 32, 335706.	1.3	2
9	Adjusting the electronic structure of WS2 nanosheets by iron doping to promote hydrogen evolution reaction. FlatChem, 2021, 29, 100278.	2.8	2
10	Surface-Electronic-Structure Reconstruction of Perovskite via Double-Cation Gradient Etching for Superior Water Oxidation. Nano Letters, 2021, 21, 8166-8174.	4.5	29
11	Cation substitution of B-site in LaCoO3 for bifunctional oxygen electrocatalytic activities. Journal of Alloys and Compounds, 2021, 878, 160433.	2.8	25
12	Multi-stability modulating of alkaline-earth metal doped LaCoO3 for rechargeable Zn-air batteries. Energy Storage Materials, 2021, 42, 470-476.	9.5	22
13	High-valent Zirconium-doping modified Co3O4 weave-like nanoarray boosts oxygen evolution reaction. Journal of Alloys and Compounds, 2021, 886, 161172.	2.8	26
14	Ferromagnetism of two-dimensional transition metal chalcogenides: both theoretical and experimental investigations. Nanoscale, 2021, 13, 12772-12787.	2.8	12
15	Hydrogen-etched CoS ₂ to produce a Co ₉ S ₈ @CoS ₂ heterostructure electrocatalyst for highly efficient oxygen evolution reaction. RSC Advances, 2021, 11, 30448-30454.	1.7	12
16	Tunable ferromagnetic ordering in phosphorus adsorbed ReS2 nanosheets. Nanotechnology, 2021, 32, 075701.	1.3	2
17	Energy-level engineered hollow N-doped NiS1.03 for Zn–Air batteries. Energy Storage Materials, 2020, 25, 202-209.	9.5	62
18	Robust ferromagnetism in Cr-doped ReS ₂ nanosheets demonstrated by experiments and density functional theory calculations. Nanotechnology, 2020, 31, 175702.	1.3	7

#	Article	IF	CITATIONS
19	Engineering Lower Coordination Atoms onto NiO/Co ₃ O ₄ Heterointerfaces for Boosting Oxygen Evolution Reactions. ACS Catalysis, 2020, 10, 12376-12384.	5.5	223
20	High efficiency electrocatalyst of LaCr0.5Fe0.5O3 nanoparticles on oxygen-evolution reaction. Scientific Reports, 2020, 10, 13395.	1.6	17
21	Giant magnetoelectric coupling observed at high frequency in NiFe ₂ O ₄ –BaTiO ₃ particulate composite. RSC Advances, 2020, 10, 27242-27248.	1.7	10
22	Enhanced thermal stability of lead-free (1-x)Ba(Zr0.2Ti0.8)O3-x(Ba0.7Ca0.3)TiO3 ferroelectric ceramics. Journal of Materials Science, 2020, 55, 16890-16899.	1.7	6
23	A Co ₃ O ₄ /MnCO ₃ heterojunction on three-dimensional nickel foam for an enhanced oxygen evolution reaction. CrystEngComm, 2020, 22, 3984-3990.	1.3	7
24	Aliovalent fluorine doping and anodization-induced amorphization enable bifunctional catalysts for efficient water splitting. Journal of Materials Chemistry A, 2020, 8, 10831-10838.	5.2	31
25	Engineered spin state in Ce doped LaCoO3 with enhanced electrocatalytic activity for rechargeable Zn-Air batteries. Nano Energy, 2020, 74, 104948.	8.2	99
26	Bifunctional Oxygen Electrocatalyst of Mesoporous Ni/NiO Nanosheets for Flexible Rechargeable Zn–Air Batteries. Nano-Micro Letters, 2020, 12, 68.	14.4	103
27	Fe-based species anchored on N-doped carbon nanotubes as a bifunctional electrocatalyst for acidic/neutral/alkaline Zn–air batteries. Nanotechnology, 2020, 31, 265402.	1.3	4
28	Modulation of Electronics of Oxide Perovskites by Sulfur Doping for Electrocatalysis in Rechargeable Zn–Air Batteries. Chemistry of Materials, 2020, 32, 3439-3446.	3.2	94
29	Electrode-controlled confinement of conductive filaments in a nanocolumn embedded symmetric–asymmetric RRAM structure. Journal of Materials Chemistry C, 2020, 8, 1577-1582.	2.7	16
30	Interfacial Engineering of NiO/NiCo ₂ O ₄ Porous Nanofibers as Efficient Bifunctional Catalysts for Rechargeable Zinc–Air Batteries. ACS Applied Materials & Interfaces, 2020, 12, 21661-21669.	4.0	80
31	Realization of "single-atom ferromagnetism―in graphene by Cu–N4 moieties anchoring. Applied Physics Letters, 2020, 116, .	1.5	9
32	Bifunctional Electrocatalytic Activity of Nitrogen-Doped NiO Nanosheets for Rechargeable Zinc–Air Batteries. ACS Applied Materials & Interfaces, 2019, 11, 30865-30871.	4.0	41
33	Structural distortion induced ferromagnetism in two-dimensional metal-free graphitic-C ₃ N ₄ nanosheets. RSC Advances, 2019, 9, 21391-21395.	1.7	9
34	Bifunctional catalysts of CoNi nanoparticle-embedded nitrogen-doped carbon nanotubes for rechargeable Zn–air batteries. Nanotechnology, 2019, 30, 435701.	1.3	20
35	Special atmosphere annealed Co3O4 porous nanoclusters with oxygen defects and high proportion of Co2+ for oxygen evolution reaction. Journal of Alloys and Compounds, 2019, 806, 163-169.	2.8	24
36	N ⁺ -ion irradiation engineering towards the efficient oxygen evolution reaction on NiO nanosheet arrays. Journal of Materials Chemistry A, 2019, 7, 4729-4733.	5.2	48

#	Article	IF	CITATIONS
37	Electronic structure modulation of NiS ₂ by transition metal doping for accelerating the hydrogen evolution reaction. Journal of Materials Chemistry A, 2019, 7, 4971-4976.	5.2	93
38	Co and CeO ₂ co-decorated N-doping carbon nanofibers for rechargeable Zn–air batteries. Nanotechnology, 2019, 30, 395401.	1.3	37
39	Defect-related high temperature ferromagnetism in mechanically milled hexagonal boron nitride nanoplates. Applied Surface Science, 2019, 487, 825-832.	3.1	10
40	Cu and Co nanoparticle-Co-decorated N-doped graphene nanosheets: a high efficiency bifunctional electrocatalyst for rechargeable Zn–air batteries. Journal of Materials Chemistry A, 2019, 7, 12851-12858.	5.2	50
41	Bifunctional porous Co-doped NiO nanoflowers electrocatalysts for rechargeable zinc-air batteries. Applied Catalysis B: Environmental, 2019, 250, 71-77.	10.8	98
42	Phosphorus dual-site driven CoS ₂ @S, N co-doped porous carbon nanosheets for flexible quasi-solid-state supercapacitors. Journal of Materials Chemistry A, 2019, 7, 26618-26630.	5.2	82
43	Zn-doped MoSe2 nanosheets as high-performance electrocatalysts for hydrogen evolution reaction in acid media. Electrochimica Acta, 2019, 296, 701-708.	2.6	70
44	Bimetallic Nickel Cobalt Sulfide as Efficient Electrocatalyst for Zn–Air Battery and Water Splitting. Nano-Micro Letters, 2019, 11, 2.	14.4	179
45	Dualâ€Native Vacancy Activated Basal Plane and Conductivity of MoSe ₂ with Highâ€Efficiency Hydrogen Evolution Reaction. Small, 2018, 14, e1704150.	5.2	114
46	Accelerated Hydrogen Evolution Reaction in CoS ₂ by Transition-Metal Doping. ACS Energy Letters, 2018, 3, 779-786.	8.8	231
47	Durable oxygen evolution reaction of one dimensional spinel CoFe ₂ O ₄ nanofibers fabricated by electrospinning. RSC Advances, 2018, 8, 5338-5343.	1.7	54
48	Selfâ€Powered Waterâ€Splitting Devices by Core–Shell NiFe@Nâ€Graphiteâ€Based Zn–Air Batteries. Advan Functional Materials, 2018, 28, 1706928.	ced.8	155
49	TMD-based highly efficient electrocatalysts developed by combined computational and experimental approaches. Chemical Society Reviews, 2018, 47, 4332-4356.	18.7	232
50	Activation of the MoSe ₂ basal plane and Se-edge by B doping for enhanced hydrogen evolution. Journal of Materials Chemistry A, 2018, 6, 510-515.	5.2	110
51	Facile one-step synthesis of phosphorus-doped CoS2 as efficient electrocatalyst for hydrogen evolution reaction. Electrochimica Acta, 2018, 259, 955-961.	2.6	92
52	Re doping induced 2H-1T phase transformation and ferromagnetism in MoS2 nanosheets. Applied Physics Letters, 2018, 113, .	1.5	45
53	Transition-metal-doped NiSe2 nanosheets towards efficient hydrogen evolution reactions. Nano Research, 2018, 11, 6051-6061.	5.8	72
54	A low crystallinity oxygen-vacancy-rich Co ₃ O ₄ cathode for high-performance flexible asymmetric supercapacitors. Journal of Materials Chemistry A, 2018, 6, 16094-16100.	5.2	182

#	Article	IF	CITATIONS
55	Integrated Hierarchical Carbon Flake Arrays with Hollow Pâ€Doped CoSe ₂ Nanoclusters as an Advanced Bifunctional Catalyst for Zn–Air Batteries. Advanced Functional Materials, 2018, 28, 1804846.	7.8	192
56	Activation of defective nickel molybdate nanowires for enhanced alkaline electrochemical hydrogen evolution. Nanoscale, 2018, 10, 16539-16546.	2.8	29
57	Ar ²⁺ Beam Irradiation-Induced Multivancancies in MoSe ₂ Nanosheet for Enhanced Electrochemical Hydrogen Evolution. ACS Energy Letters, 2018, 3, 2167-2172.	8.8	73
58	P Dopants Triggered New Basal Plane Active Sites and Enlarged Interlayer Spacing in MoS ₂ Nanosheets toward Electrocatalytic Hydrogen Evolution. ACS Energy Letters, 2017, 2, 745-752.	8.8	304
59	Activating and Optimizing Activity of CoS ₂ for Hydrogen Evolution Reaction through the Synergic Effect of N Dopants and S Vacancies. ACS Energy Letters, 2017, 2, 1022-1028.	8.8	229
60	P dopants induced ferromagnetism in g-C3N4 nanosheets: Experiments and calculations. Applied Physics Letters, 2017, 110, .	1.5	25
61	Phase-transfer induced room temperature ferromagnetic behavior in 1T@2H-MoSe2 nanosheets. Scientific Reports, 2017, 7, 45307.	1.6	23
62	Dualâ€Functional N Dopants in Edges and Basal Plane of MoS ₂ Nanosheets Toward Efficient and Durable Hydrogen Evolution. Advanced Energy Materials, 2017, 7, 1602086.	10.2	286
63	Copper dopants improved the hydrogen evolution activity of earth-abundant cobalt pyrite catalysts by activating the electrocatalytically inert sulfur sites. Journal of Materials Chemistry A, 2017, 5, 17601-17608.	5.2	61
64	Adjustable ferromagnetic behavior in iron-doped two-dimensional MoS ₂ multilayer nanosheets. Applied Physics Express, 2017, 10, 093002.	1.1	21
65	Anion vacancy-mediated ferromagnetism in atomic-thick Ni3N nanosheets. Applied Physics Letters, 2017, 111, .	1.5	11
66	High temperature ferromagnetism in Cu-doped MoS ₂ nanosheets. Journal Physics D: Applied Physics, 2016, 49, 165003.	1.3	65
67	Metallic Ni ₃ N nanosheets with exposed active surface sites for efficient hydrogen evolution. Journal of Materials Chemistry A, 2016, 4, 17363-17369.	5.2	233
68	Enhanced Catalytic Activities of Metal-Phase-Assisted 1T@2H-MoSe 2 Nanosheets for Hydrogen Evolution. Electrochimica Acta, 2016, 217, 181-186.	2.6	83
69	Atomically Thin B doped g-C3N4 Nanosheets: High-Temperature Ferromagnetism and calculated Half-Metallicity. Scientific Reports, 2016, 6, 35768.	1.6	74
70	N-doped WS ₂ nanosheets: a high-performance electrocatalyst for the hydrogen evolution reaction. Journal of Materials Chemistry A, 2016, 4, 11234-11238.	5.2	147
71	Argon ion irradiation induced phase transition and room temperature ferromagnetism in the CuO thin film. Journal Physics D: Applied Physics, 2016, 49, 055003.	1.3	7
72	Green synthesis of Pt–Au dendrimer-like nanoparticles supported on polydopamine-functionalized graphene and their high performance toward 4- nitrophenol reduction. Applied Catalysis B: Environmental, 2016, 181, 371-378.	10.8	343

#	Article	IF	CITATIONS
73	Cu vacancies modulated the room temperature ferromagnetism in Cu ₂ O/Cu nanoparticle composites. CrystEngComm, 2015, 17, 2118-2122.	1.3	9
74	Zigzag-edge related ferromagnetism in MoSe ₂ nanoflakes. Physical Chemistry Chemical Physics, 2015, 17, 32505-32510.	1.3	26
75	Manifestation of high-temperature ferromagnetism in fluorinated graphitic carbon nitride nanosheets. Journal of Materials Chemistry C, 2015, 3, 12230-12235.	2.7	21
76	Tunable ferromagnetic ordering in MoS ₂ nanosheets with fluorine adsorption. Nanoscale, 2015, 7, 4211-4216.	2.8	65
77	Enhanced hydrogen evolution catalysis in MoS ₂ nanosheets by incorporation of a metal phase. Journal of Materials Chemistry A, 2015, 3, 24414-24421.	5.2	88
78	Abnormal room temperature ferromagnetism in CuO–ZnO heterostructures: interface related or not?. Chemical Communications, 2015, 51, 1151-1153.	2.2	16
79	Realization of high Curie temperature ferromagnetism in atomically thin MoS ₂ and WS ₂ nanosheets with uniform and flower-like morphology. Nanoscale, 2015, 7, 650-658.	2.8	94
80	Ferromagnetism in ultrathin MoS2 nanosheets: from amorphous to crystalline. Nanoscale Research Letters, 2014, 9, 586.	3.1	63
81	Room temperature ferromagnetism in Zn0.99La0.01O and pure ZnO nanoparticles. Materials Chemistry and Physics, 2014, 145, 510-514.	2.0	7
82	Observation of room temperature ferromagnetism in pure La2O3 nanoparticles. Applied Physics A: Materials Science and Processing, 2014, 116, 1293-1298.	1.1	15
83	Porous tin disulfide nanosheets with room temperature ferromagnetic nature. CrystEngComm, 2014, 16, 7876.	1.3	23
84	A series of unexpected ferromagnetic behaviors based on the surface-vacancy state: an insight into NiO nanoparticles with a core–shell structure. RSC Advances, 2014, 4, 46133-46140.	1.7	34
85	Defect-related ferromagnetism in ultrathin metal-free g-C3N4 nanosheets. Nanoscale, 2014, 6, 2577.	2.8	167
86	Enhancing the catalytic activity of flowerike Pt nanocrystals using polydopamine functionalized graphene supports for methanol electrooxidation. Electrochimica Acta, 2014, 142, 18-24.	2.6	70
87	Ferromagnetism in ultrathin VS2 nanosheets. Journal of Materials Chemistry C, 2013, 1, 5909.	2.7	149
88	Magnetic resonance of the NiFe2O4 nanoparticles in the gigahertz range. Nanoscale Research Letters, 2013, 8, 404.	3.1	27
89	Ferromagnetism in exfoliated tungsten disulfide nanosheets. Nanoscale Research Letters, 2013, 8, 430.	3.1	97
90	Ferromagnetism in freestanding MoS2 nanosheets. Nanoscale Research Letters, 2013, 8, 129.	3.1	180

#	Article	IF	CITATIONS
91	Coexistence of ferromagnetism and spin glass behavior in antiferromagnetic Y2BaCuO5. Physica C: Superconductivity and Its Applications, 2013, 490, 32-36.	0.6	1
92	Ferromagnetism in sphalerite and wurtzite CdS nanostructures. Nanoscale Research Letters, 2013, 8, 17.	3.1	33
93	Interface mediated ferromagnetism in bulk CuO/Cu2O composites. Applied Physics Letters, 2012, 101, .	1.5	23
94	Room temperature ferromagnetism in pure Y 2 O 3 nanoparticles. Europhysics Letters, 2012, 97, 17005.	0.7	11
95	<i>d</i> ferromagnetism in undoped sphalerite ZnS nanoparticles. Applied Physics Letters, 2011, 99, .	1.5	71
96	Ferromagnetism Induced by Oxygen Vacancies in Zinc Peroxide Nanoparticles. Journal of Physical Chemistry C, 2011, 115, 16405-16410.	1.5	35
97	Transforming from paramagnetism to room temperature ferromagnetism in CuO by ball milling. AIP Advances, 2011, 1, .	0.6	19
98	Synthesis and magnetic properties of Zr doped ZnO Nanoparticles. Nanoscale Research Letters, 2011, 6, 587.	3.1	57
99	Effect of annealing temperature on the magnetic properties of Zn _{0.97} Al _{0.03} O nanoparticles. Physica Status Solidi (A) Applications and Materials Science, 2011, 208, 2454-2459.	0.8	2
100	Ferromagnetism in ZnO Nanoparticles Induced by Doping of a Nonmagnetic Element: Al. Journal of Physical Chemistry C, 2010, 114, 13477-13481.	1.5	111
101	Magnetic properties of Er-doped ZnO films prepared by reactive magnetron sputtering. Applied Physics A: Materials Science and Processing, 2010, 100, 79-82.	1.1	37
102	Vacancy-Mediated Magnetism in Pure Copper Oxide Nanoparticles. Nanoscale Research Letters, 2010, 5, 769-772.	3.1	171
103	Synthesis, Magnetic Anisotropy and Optical Properties of Preferred Oriented Zinc Ferrite Nanowire Arrays. Nanoscale Research Letters, 2010, 5, 1289-1294.	3.1	87
104	Room-Temperature Ferromagnetism of Flowerlike CuO Nanostructures. Journal of Physical Chemistry C, 2010, 114, 18347-18351.	1.5	163
105	Defect-Mediated Magnetism in Pure CaO Nanopowders. Journal of Physical Chemistry C, 2010, 114, 11703-11707.	1.5	45
106	Room Temperature Ferromagnetism in Vacuum-Annealed CoO Nanospheres. Journal of Physical Chemistry C, 2010, 114, 21989-21993.	1.5	66
107	Room temperature ferromagnetism of Cu doped ZnO nanowire arrays. Journal of Applied Physics, 2009, 105, .	1.1	34
108	Room-temperature ferromagnetism in Er-doped ZnO thin films. Scripta Materialia, 2009, 60, 289-292.	2.6	58

#	Article	IF	CITATIONS
109	Room temperature ferromagnetism of pure ZnO nanoparticles. Journal of Applied Physics, 2009, 105, .	1.1	178
110	The influences of electrodeposited temperature on the morphology and magnetic properties of Fe/Fe–dimethylsulfoxide nanocables. Electrochimica Acta, 2008, 53, 5464-5468.	2.6	11
111	Preparation and magnetic properties of Nd5Fe95â^'xBx nanowire arrays. Materials Letters, 2008, 62, 3070-3072.	1.3	20